

Received 10 July 2020; revised 2 October 2020; accepted 4 October 2020. Date of publication 6 October 2020; date of current version 21 October 2020. The review of this article was arranged by Editor C. C. McAndrew.

Digital Object Identifier 10.1109/JEDS.2020.3029184

Investigation of THz Frequency Shaped Anode Planar Gunn Diodes Operating in Delayed Mode

AHMED MINDIL¹, GEOFFREY DUNN¹, ATA KHALID², AND CHRIS OXLEY³

¹ School of Natural and Computing Sciences, College of Physical Sciences, University of Aberdeen, Aberdeen AB24 3UE, U.K.
² Centre of Electronic Warfare, Information and Cyber, Cranfield University, Defence Academy of the United Kingdom, Shrivenham SN6 8LA, U.K.
³ School of Engineering and Sustainable Development, De Montfort University, Leicester LE1 9BH, U.K.

CORRESPONDING AUTHOR: A. MINDIL (e-mail: r01amhm@abdn.ac.uk)

This work was supported by Saudi Arabia's Ministry of Higher Education.

ABSTRACT A novel planar design of Gunn diode with a shaped anode contact, utilizing Monte Carlo simulations, has been shown to have produced 0.3 THz frequency current output when operated in delayed mode. Two novel anode designs are investigated here, one with two fixed distances, and the other with three fixed distances between the cathode and anode electrodes. The corresponding waveforms generated, show two and three current peaks respectively. The work suggests high frequency and novel wave-shaping applications are possible in such devices.

INDEX TERMS Gallium arsenide, THz frequency, multiple peaks, Monte Carlo simulation, delayed mode, planar Gunn device.

I. INTRODUCTION

Gunn devices, or transferred electron devices (TED), are two-terminal negative differential resistance (NDR) devices that generate RF power which have been popular since the 1970s as a microwave frequency source [1]–[3]. Most research into these devices has concentrated on vertical structures and comparatively few researchers have explored planar architectures. These structures offer significant advantages over vertical structures as they are more easily incorporated within Microwave Monolithic Integrated Circuits (MMIC's) also the natural frequency of these devices is controlled by the fabrication rather than the material epitaxial growth process. The development of the planar diode [4]–[13] has shown many of the expected advantages of these devices, however the RF power output has remained disappointing low. Therefore, in recent years, the critical challenge of planar Gunn devices has been to further improve the RF output power and the oscillation frequency into the sub-terahertz region [14]. However, the short transit region required for high frequency operation will limit the magnitude of the bias voltage that can be applied before the device breaks down.

Planar Gunn diodes have been proved to function at high frequencies, as demonstrated for a $\text{In}_{0.53}\text{Ga}_{0.47}\text{As}$ planar Gunn diode [15]. This device, with a 0.6 μm channel length,

operated at a fundamental frequency above 300 GHz and by using other material systems showed the potential of operating into the THz region [16]. Recent work [17] has shown an alternative approach to obtain higher frequencies without relying on fabricating very short transit regions, by shaping the anode and cathode contacts. Using this approach domains incident on a shaped anode, can produce multiple current peaks as the domain hits the different parts of the anode at different times. This idea was explored in [17] for diodes operating in both natural (with constant DC bias) and in a delayed mode (where an RF feedback bias is sufficient to lower the potential below the threshold for domain formation). It was found that an elaborate design of the anode and cathode geometry was required to sustain repeated oscillations. With a constant DC bias there was a tendency for the domain to become chaotic. However, in delayed mode, because the domain is extinguished after each transit, there would be no memory of previous transits and so the tendency of chaotic oscillations is effectively dealt with.

In this article, an ensemble Monte Carlo simulation has been performed on three structures of the planar Gunn diode, one of which is a single transit region structure for comparison. We will demonstrate the different designs produce stable and repeated domains that yield a simple current waveform

with multiple peaks which correspond to every transit of the domain.

II. DEVICE STRUCTURE AND SIMULATION METHOD

An ensemble Monte Carlo method was used to simulate the carrier transport in the studied GaAs devices with an established 2-D Ensemble Monte Carlo (EMC) transport model [19], which has been validated against several related devices performed experimentally [12], [13]. As previously, in [17], [18], in order to simulate the effect of the cathode contact, a doping notch was employed to precipitate domain formation. In this structure, up to 150,000 super particles were used with a standard mesh of 100 by 100. A field adjusting time step of 1 fs was utilized and the boundary conditions adopted were the usual Dirichlet conditions for the contacts with defined potentials and Neumann conditions at other boundaries assuming continuity of the electric field. The simulations were considered as valid provided that the electric field and domain were normal for the lower boundary, going down along the unstimulated part of the channel. Due to the noise in a Monte Carlo simulation, it is difficult to link a Monte Carlo model with the external circuit model [20], so in the case of devices in a tuned circuit is assumed that steady-state oscillations have been established and the device experiences a RF voltage V_{RF} such that $V = V_{DC} + V_{RF}\sin(\omega t)$ [20]–[22].

Figure 1 shows a schematic illustration of the three simulated devices. In 1b and 1c details of the anode design showing a crenellated structure where the merlons have a mushroom form. As in [17], this is to prevent the domain wrapping around the merlon and so increase the distinctness of the domain contacting the merlon and next subsequently the crenel producing an increase in current at each contact. For ease and accuracy of simulation, we only simulated a unit cell of $14\mu\text{m}$ width of the channel length (see Figure 1). The channel was $1.6\mu\text{m}$ from anode to cathode, for the conventional planar Gunn structure (Figure 1a), ranging from 1.3 to $1.6\mu\text{m}$ for the non-uniform active channel (first novel structure shown in Figure 1b) and 1, 1.3 and $1.6\mu\text{m}$ for the second novel structure (Figures 1c). The simulations were done on the assumption of functional operation in an optimized device with a uniform lattice temperature of 300 K (room temperature) and at a DC bias of 2V with RF feedback of 1V.

III. RESULT AND DISCUSSIONS

The current response to the 45 GHz (22ps period) applied potential for each device is shown in Figure 2. In order to understand the waveform, it is useful to start with the conventional design and then observe the embroidering of the current waveform by the additional structure of the anode in the other devices.

A. CONVENTIONAL DESIGN

As this is a delayed mode of oscillation, there will be two peaks of current in each cycle, the first of these will be

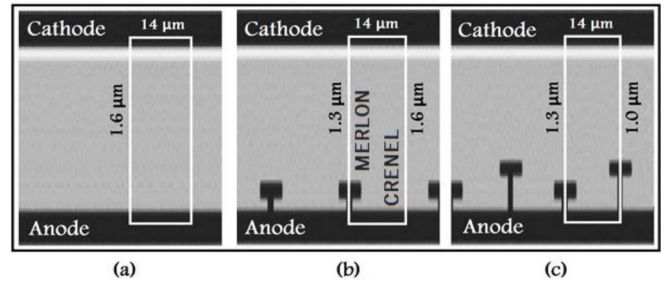


FIGURE 1. (a) Schematic of the conventional device with straight contacts spacing of $1.6\mu\text{m}$, (b) Schematic of the straight cathode with non-uniform anode contacts spacing of 1.6 and $1.3\mu\text{m}$, (c) Schematic of the straight cathode with different non-uniform anode contacts spacing of 1.6, 1.3, and $1.0\mu\text{m}$.

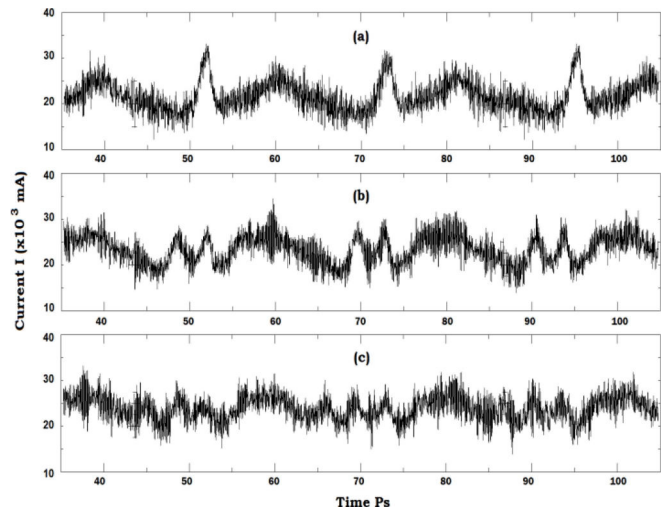


FIGURE 2. Total current from Monte Carlo simulation of (a) a conventional planar Gunn diode, (b) a crenellated design with two different distances between contacts, and (c) a crenellated design with three different distances between contacts.

due to the contact of the domain with the anode and reformation of a new domain at the cathode. However, after this, as the applied potential falls below the threshold voltage for domain formation the current will fall and this new domain will be extinguished. The second peak is caused by the increase in voltage and the creation of a fresh domain. After this, the current falls again with further increases in voltage as the domain travels to the anode. In terms of our device then, the current in Figure 2a at 45ps, corresponds to the domain travelling toward the anode. Here the current is gradually reducing, going down into a trough at 48ps. The domain is then incident on the anode contact and a new domain begins to reform at the cathode; this corresponds to the current peak at 52 ps. After the domain has passed through the anode and started to reform at the cathode, the feedback potential drops below threshold extinguishing the domain and the current consequently falls. As the voltage rises again, there is a corresponding rise in the current as we move towards the 60ps peak (differential resistivity is positive here). The voltage then becomes sufficient for a new

domain to form and the current then starts to reduce (differential resistivity becomes negative again). The process then repeats with the next transit of the domain and and at 65ps the domain has reformed and is travelling toward the anode.

B. SINGLE MERLON HEIGHT

Figure 2b shows the current form from the device design shown in Figure 1b. The broad structure of the current can be seen to be the same as in 2a, however the single peak is now broken into two peaks 3.3ps apart (0.3THz). As before the domain at 65ps is making its way toward the anode. Next, the domain is incident on the anode merlon causing the first peak at 69.7 ps in the current. The current falls for the following 3.3ps as the remaining part of the domain moves toward the crenel. When the domain makes contact with the crenel at 73ps, the current increases again (with the merlon component of the domain having already reformed and progressing through the transit region). Next, as the applied voltage falls under the threshold voltage all parts of the domain are extinguished. Subsequently, when the voltage rises once again, the current raises as before and a new domain forms and is in transit within the channel at 85ps.

C. DOUBLE MERLON HEIGHT

The dynamics of the double merlon height design are quite complicated and Figures 3 (I-VI) presents the simulated electron densities at 66, 69.3, 72.6, 78, 80, and 82ps respectively. These time points were chosen to best illustrate the various stages of the cycle. As in the previous two devices, the domain has formed and is travelling toward the anode at 64ps until at 66ps it is incident on the high merlon (see Figure 3.I and the first current peak in Figure 2c). The current in Figure 2c then decreases as the domain moves onwards to hit the second low merlon (see Figure 3.II and the second peak in current in Figure 2c at 69.3ps). Note that the new domain corresponding to the highest merlon has reformed at the cathode and is transiting the channel again. In this way as each part of the domain passes out of the anode, the new domain forms at the cathode, so that the new domain will reflect the shape of the anode. At 72.6ps (Figure 3 III), a number of things are happening which need explanation. Firstly, subsequent to the old domain passing through the low merlon, a new domain has formed and is in transit. Secondly, the old domain is hitting the crenel of the anode and the new domain from the high merlon is also hitting the high merlon at the same time causing a peak in current in Figure 2c at this time.

Note that careful choice of the height of the high merlon has allowed for this coincidental timing, other choices would split this current peak into a further fine structure. Figure 3 IV shows a new, continuous but weakened and distorted domain in the channel at 78ps. The potential having fallen below threshold the domain is extinguished and at 80ps (Figure 3 V) the current is increasing again (due to an increasing potential and positive differential resistivity).

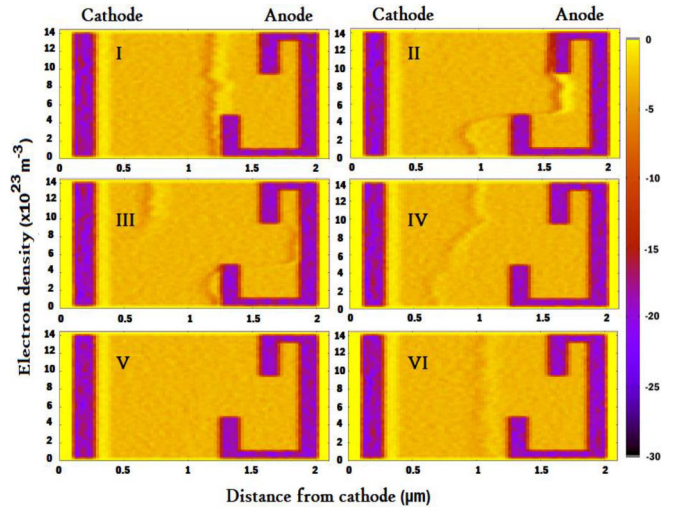


FIGURE 3. (I-VI), shows the density of the electrons with an 1.5 V bias at different times. (I) The domain contacts the first merlons at 66ps. (II) 3.3ps later, the domain reaches the second merlon. (III) The domain reaches the crenel after another 3.3ps. (IV) At 78 ps, the new and distorted domain is formed. (v) Because of the falling voltage at 80 ps, the domain is extinguished. (VI) At 82 ps, the domain reforms.

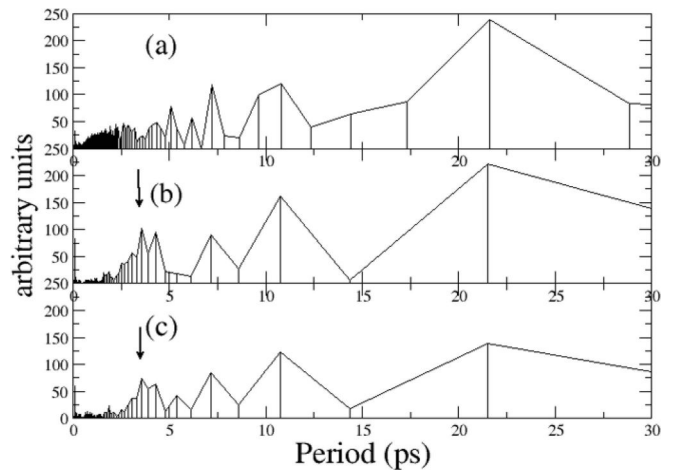


FIGURE 4. Frequency spectrum of current response of the conventional device (4a), the single merlon device (4b) and the double merlon device (4c). The arrow indicates the 3.3ps fine structure.

Finally, the potential becomes sufficient for a new fresh and straight domain to form at the cathode (shown in transit at 82ps in Figure 3 VI) and the peak in current in Figure 2c.

Figures 4a, b and c show the transformed frequency spectrum of the currents in Figures 2a, b and c respectively. Figure 4a shows the spectrum for the conventional device and this overall pattern is repeated in Figures 4b and 4c. It can be seen that the magnitude of the components, for example at 22ps are hardly affected in the single merlon device, though they are reduced by about 40% in the double merlon device. However, in 4b and 4c, the frequency spectrum is augmented by strong peaks around the 3.3ps periods discussed earlier.

Operating a Gunn diode in its delayed mode allows a series resonant circuit to be used and vertical Gunn diodes operating in this mode have achieved good efficiencies at the extracted harmonic [23]. The planar nature of the planar Gunn diode will enable it to be fabricated using MMIC technology and the enhanced harmonic current characteristics of the diode should enable efficient operation to be achievable into the millimetric and THz frequency bands. Planar Gunn diodes have the benefit of being able to be fabricated with different transit lengths and therefore different operating frequencies on the same substrate, thereby opening up new applications.

IV. CONCLUSION

Based on the simulation Monte Carlo, we have investigated fine structure in the output current of GaAs planar Gunn diodes caused by novel anode contact designs. Our simulated results confirm that shaped contacts can generate stable cyclic Gunn domain transits that will produce a current with high frequency components much greater than the nominal domain transit time. The embroidering of the current wave form of the conventional device, is controlled by the number of merlons; two peaks in the single merlon device and the three peaks in the double merlon device. The period was chosen to be 3.3ps corresponding to the time of transit of a domain across the 0.3 micron step size between the merlons and crenels. Higher frequencies should be possible by reducing the step size, though the distinctness of the peaks is likely to reduce.

As the design of the anode contact becomes more complex, the domain formation and reformation in different parts of the device becomes correspondingly convoluted with some parts of the device supporting several domain transits during only one transit in another part of the device. This in turn can lead to evermore elaborate embroidering of the basic waveform.

In conclusion, a new geometrical structure of contacts for a planar Gunn diode has been presented, which create the multiple peaks of the domain, and these designs lead to well-ordered domain peaks. Embedding the device in a tuned circuit to extract the enhanced harmonic may lead to low cost MMIC milli-metric and THz RF sources for a wide range of applications. As well, the capability of changing the profile of waveforms by the design of the contacts may have many different waveform shaping possibilities.

ACKNOWLEDGMENT

The authors thank the University of Aberdeen for providing the necessary support.

REFERENCES

- [1] P. J. Bulman, G. S. Hobson, and B. C. Taylor, *Transferred Electron Devices*. New York, NY, USA: Academic, Inc., 1972, p. 402.
- [2] S. M. Sze, *Modern Semiconductor Device Physics*. New York, NY, USA: Wiley Inc., 1998.
- [3] J. B. Gunn, "Microwave oscillations of current in III-V semiconductors," *Solid-State Commun.*, vol. 1, no. 4, pp. 88–91, 1963, doi: [10.1016/0038-1098\(63\)90041-3](https://doi.org/10.1016/0038-1098(63)90041-3).
- [4] Y. Lechaux *et al.*, "Comprehensive characterization of gunn oscillations in In_{0.53}Ga_{0.47}As planar diodes," *Semicond. Sci. Technol.*, vol. 35, no. 11, 2020, Art. no. 115009, doi: [10.1088/1361-6641/abab1f](https://doi.org/10.1088/1361-6641/abab1f).
- [5] J. Mateos *et al.*, "Design and fabrication of planar gunn nanodiodes based on doped GaN," in *Proc. IEEE Asia-Pac. Microw. Conf. (APMC)*, Singapore, 2019, pp. 971–973, doi: [10.1109/APMC46564.2019.9038486](https://doi.org/10.1109/APMC46564.2019.9038486).
- [6] M. Maricar *et al.*, "An electrical equivalent circuit to simulate the output power of an AlGaAs/GaAs planar gunn diode oscillator," *Microw. Opt. Technol. Lett.*, vol. 60, no. 9, pp. 2144–2148, 2018. [Online]. Available: <https://doi.org/10.1002/mop.31312>
- [7] E. S. Obolenskaya, E. A. Tarasova, A. Y. Churin, S. V. Obolensky, and V. A. Kozlov, "Microwave-signal generation in a planar Gunn diode with radiation exposure taken into account," *Semiconductors*, vol. 50, pp. 1579–1583, Feb. 2017. [Online]. Available: <https://doi.org/10.1134/S1063782616120149>
- [8] Y. Wang, L. Yang, Z. Wang, and Y. Hao, "Modulation of the domain mode in GaN-based planar Gunn diode for terahertz applications," *Physica Status Solidi*, vol. 13, pp. 382–385, May 2016.
- [9] M. Maricar, A. Khalid, D. Cumming, and C. Oxley, "Extraction of second harmonic from an InP based planar Gunn diode using diamond resonator for milli-metric wave frequencies," *Solid-State Electron.*, vol. 116, pp. 104–106, Feb. 2016. [Online]. Available: <https://doi.org/10.1016/j.sse.2015.12.001>
- [10] A. Khalid, C. Li, V. Papageorgiou, N. J. Pilgrim, G. M. Dunn, and D. R. S. Cumming, "A 218-GHz second-harmonic multiquantum well GaAs-based planar Gunn diodes," *Microw. Opt. Technol. Lett.*, vol. 55, no. 3, pp. 686–688, 2013, doi: [10.1002/mop.27393](https://doi.org/10.1002/mop.27393).
- [11] L. Chong, "Design and characterisation of millimetre wave planar gunn diodes and integrated circuits," Ph.D. dissertation, Dept. Doctoral, Univ. Glasgow, Glasgow, U.K., 2012.
- [12] A. Khalid *et al.*, "A planar gunn diode operating above 100 GHz," *IEEE Electron Device Lett.*, vol. 28, no. 10, pp. 849–851, Oct. 2007, doi: [10.1109/LED.2007.904218](https://doi.org/10.1109/LED.2007.904218).
- [13] W. H. Haydl, "Planar Gunn diodes with ideal contact geometry," *Proc. IEEE*, vol. 61, no. 4, p. 497, Apr. 1973, doi: [10.1109/PROC.1973.9090](https://doi.org/10.1109/PROC.1973.9090).
- [14] A. Mindil, G. M. Dunn, A. Khalid, and C. H. Oxley, "Investigation of contact edge effects in the channel of planar gunn diodes," *IEEE Trans. Electron Devices*, vol. 67, no. 1, pp. 53–56, Jan. 2020, doi: [10.1109/TED.2019.2951301](https://doi.org/10.1109/TED.2019.2951301).
- [15] A. Khalid *et al.*, "Terahertz oscillations in an In_{0.53}Ga_{0.47}As submicron planar Gunn diode," *J. Appl. Phys.*, vol. 115, no. 11, Mar. 2014, Art. no. 114502, doi: [10.1063/1.4868705](https://doi.org/10.1063/1.4868705).
- [16] S. Pérez, T. González, D. Pardo, and J. Mateos, "Terahertz Gunn-like oscillations in InGaAs/InAlAs planar diodes," *J. Appl. Phys.*, vol. 103, no. 9, pp. 1–5, May 2008, doi: [10.1063/1.2917246](https://doi.org/10.1063/1.2917246).
- [17] A. Mindil, G. M. Dunn, A. Khalid, and C. H. Oxley, "Investigation of high-frequency fine structure in the current output of shaped contact planar Gunn diodes," *IEEE Trans. Electron Devices*, vol. 67, no. 5, pp. 1946–1951, May 2020, doi: [10.1109/TED.2020.2981191](https://doi.org/10.1109/TED.2020.2981191).
- [18] N. J. Pilgrim, A. Khalid, C. Li, G. M. Dunn, and D. R. S. Cumming, "Contact shaping in planar gunn diodes," *Physica Status Solidi*, vol. 8, no. 2, pp. 313–315, 2011, doi: [10.1002/pssc.201000539](https://doi.org/10.1002/pssc.201000539).
- [19] M. V. Fischetti, "Monte-Carlo simulation of transport in technologically significant semiconductors of the diamond and zinc-blende structures. I. Homogeneous transport," *IEEE Trans. Electron Devices*, vol. 38, no. 3, pp. 634–649, Mar. 1991, doi: [10.1109/16.75176](https://doi.org/10.1109/16.75176).
- [20] R. Kamoua, "Monte-Carlo-based harmonic-balance technique for the simulation of high-frequency TED oscillators," *IEEE Trans. Microw. Theory Techn.*, vol. 46, no. 10, pp. 1376–1381, Oct. 1998, doi: [10.1109/22.721138](https://doi.org/10.1109/22.721138).
- [21] R. Kamoua, H. Eisele, and G. I. Haddad, "D-band (110–170 GHz) InP Gunn devices," *Solid-State Electron.*, vol. 36, no. 11, pp. 1547–1555, 1993, doi: [10.1016/0038-1101\(93\)90026-M](https://doi.org/10.1016/0038-1101(93)90026-M).
- [22] R. Judaschke, "Comparison of modulated impurity-concentration InP transferred electron devices for power generation at frequencies above 130 GHz," *IEEE Trans. Microw. Theory Techn.*, vol. 48, no. 4, pp. 719–724, Apr. 2000, doi: [10.1109/22.841964](https://doi.org/10.1109/22.841964).
- [23] J. Carroll, *Hot Electron Microwave Generators*. Lincoln, U.K.: Hodder Stoughton Educ., 1970.